Food Chemistry: X 22 (2024) 101322

Contents lists available at ScienceDirect

Food Chemistry: X

journal homepage: www.sciencedirect.com/journal/food-chemistry-x

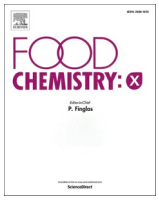

Near-infrared spectroscopy based on colorimetric sensor array coupled with convolutional neural network detecting zearalenone in wheat

Yongqin Zhao [a], Jihong Deng [a], Quansheng Chen [b,*], Hui Jiang [a,*]

[a] School of Electrical and Information Engineering, Jiangsu University, Zhenjiang 212013, China
[b] College of Ocean Food and Biological Engineering, Jimei University, Xiamen 361021, China

ARTICLE INFO

Keywords:
Wheat
Zearalenone
Colorimetric sensor array
Near-infrared spectroscopy
Convolutional neural network

ABSTRACT

Wheat is a vital global cereal crop, but its susceptibility to contamination by mycotoxins can render it unusable. This study explored the integration of two novel non-destructive detection methodologies with convolutional neural network (CNN) for the identification of zearalenone (ZEN) contamination in wheat. Firstly, the colorimetric sensor array composed of six selected porphyrin-based materials was used to capture the olfactory signatures of wheat samples. Subsequently, the colorimetric sensor array, after undergoing a reaction, was characterized by its near-infrared spectral features. Then, the CNN quantitative analysis model was proposed based on the data, alongside the establishment of traditional machine learning models, partial least squares regression (PLSR) and support vector machine regression (SVR), for comparative purposes. The outcomes demonstrated that the CNN model had superior predictive performance, with a root mean square error of prediction (RMSEP) of 40.92 μ g • kg^{-1} and a coefficient of determination on the prediction (R_P^2) of 0.91. These results affirmed the potential of integrating colorimetric sensor array with near-infrared spectroscopy in evaluating the safety of wheat and potentially other grains. Moreover, CNN can have the capacity to autonomously learn and distill features from spectral data, enabling further spectral analysis and making it a forward-looking spectroscopic tool.

1. Introduction

Wheat is a globally significant staple crop, with approximately one-third of the world's population dependent on it for sustenance (Bentley et al., 2022). In addition to providing calories and protein in the human diet, wheat also offers various vitamins and minerals (Arzani & Ashraf, 2017). Given its nutritional importance, ensuring the safety and quality of wheat is crucial (Varzakas, 2016). Specifically, the issue of fungal toxin contamination in wheat has garnered widespread attention (Sadhasivam et al., 2017). Fungal toxins have potent adverse effects and pose a threat to human health when ingested (Agriopoulou, Stamatelopoulou, & Varzakas, 2020). Zearalenone (ZEN), a naturally occurring fungal toxin, is a secondary metabolite produced by Fusarium species, commonly found in wheat and other grains. Its presence presents a challenging problem, as it not only compromises food safety and public health, but also results in economic losses in agricultural production (Ropejko & Twarużek, 2021). Currently, many countries have established minimum regulatory limits for ZEN in grains. Hence, the accurate detection of ZEN content in wheat becomes particularly critical.

In recent years, with the increasing concern for food safety, more and more researchers have focused on developing detection methods for fungal toxins (Janik et al., 2021). Currently, a significant amount of research is centered around detecting fungal toxins based on their chemical characteristics, and numerous analytical methods have been proposed for the detection of these toxins in various cereal grains. Common methods for fungal toxin detection include liquid chromatography-tandem mass spectrometry (LC/MS) (Tahoun, Gab-Allah, Yamani, & Shehata, 2021), high-performance liquid chromatography (HPLC) (Irakli, Skendi, & Papageorgiou, 2017), enzyme-linked immunosorbent assay (ELISA) (Batrinou, Houhoula, & Papageorgiou, 2020), and electrochemical-based approaches (Chen, Wu, Tang, Zhang, & Li, 2023). However, these detection methods are limited by factors such as complicated procedures, expensive equipment, and the requirement for a large amount of biochemical reagents. They are only suitable for accurate physicochemical analysis in laboratory settings and cannot achieve rapid detection of ZEN in large quantities of wheat during production, transportation, and storage. Therefore, the rapid and effective detection of ZEN content in wheat has become a research

* Corresponding authors.
E-mail addresses: chenqs@jmu.edu.cn (Q. Chen), h.v.jiang@ujs.edu.cn (H. Jiang).

https://doi.org/10.1016/j.fochx.2024.101322
Received 1 March 2024; Received in revised form 15 March 2024; Accepted 18 March 2024
Available online 21 March 2024

hotspot and an urgent issue to address.

Colorimetric sensor array, as an emerging detection technology, have found widespread applications in fields such as food, environment, and biomedicine due to their simple and convenient operation process and fast detection speed (Jiang, Deng, & Chen, 2023; Sun, Qian, Zheng, Li, & Lin, 2020; Zhao, Jiang, & Chen, 2023). These colorimetric sensors mimic the olfactory system of mammals, employing multiple color-sensitive materials as sensor units arranged in an array structure. Each sensor unit produces a distinct response to the analyte. This response is generated through strong chemical reactions, such as hydrogen bonding, metal coordination, and polar interactions, between the color-sensitive materials and the target analyte. As a result, colorimetric sensor arrays exhibit high sensitivity and are less influenced by environmental factors. By collecting the response signals from the colorimetric sensor array and processing them using computer algorithms combined with appropriate pattern recognition, differentiation and detection of multiple components in the analyte can be achieved. Currently, the feasibility of colorimetric sensor arrays has been verified in applications such as meat freshness assessment (Xu et al., 2022), tea classification and grading (Jia, Pan, Zhou, & Zhang, 2021), and grain quality evaluation (Liu, Jiang, & Chen, 2022).

However, applying this technology for quantitative detection of ZEN in moldy wheat still faces some challenges. A colorimetric sensor array captures the odor information of moldy wheat with different concentrations of ZEN, using portable instruments such as a flatbed scanner and digital camera to convert the color changes of the sensing units before and after odor response into spectral information, and obtains the corresponding values for the red, green, and blue (R, G, B) channels. By extracting the differences in the color change information of each sensor unit, i.e., the differences in red, green, and blue values (ΔR, ΔG, ΔB), the ZEN content in moldy wheat is discriminated. However, extracting three separate channel pieces of information may lead to the omission of a considerable amount of other data, which could severely limit the use and application of the colorimetric sensor array. In fact, most research on colorimetric sensor arrays remains at the qualitative differentiation stage.

Near-infrared spectroscopy is a stable and rapid detection method that captures characteristic information of samples by their absorption and scattering properties in the near-infrared band, enabling sample analysis (Pasquini, 2018). Compared to traditional analytical techniques, near-infrared spectroscopy generally does not require sample pre-treatment, is non-destructive, and has been widely used for detecting various types of samples. Additionally, near-infrared spectroscopy has a fast response rate, high analysis efficiency, and is suitable for online monitoring. Combining near-infrared spectroscopy with the colorimetric sensor array, colorimetric sensor array captures odor information of the wheat ZEN contamination, and near-infrared spectroscopy acquires the spectral information of the sensor after the wheat volatile gas reaction. Both technologies collectively detect the level of ZEN contamination in wheat. The advantages of the two technologies are combined: the colorimetric sensor array can detect the overall volatile odor of wheat, avoiding the one-sidedness of single-point spectrum collection, while the diversity of spectral data compensates for the insufficient number of variables in the colorimetric sensor array.

Chemometrics provides mathematical models for the analysis of spectral data (Mishra & Passos, 2021). However, existing chemometric spectral analysis faces the problem of decreased predictive performance of models for unknown samples. The reason for this issue is that spectral data from different sources typically contain varying background noise, and the variation in noise causes a decline in the predictive performance of previously trained models on new datasets. Spectral preprocessing and feature selection can reduce noise in spectral data and extract features to improve model accuracy. However, inappropriate spectral preprocessing and feature selection methods may introduce new errors, leading to a decrease in the model's predictive accuracy. Therefore, there is a need to develop a spectral analysis model for automatic feature extraction without the need for spectral data preprocessing and feature selection, to simplify the spectral analysis process and improve its accuracy and robustness.

Convolutional neural network (CNN) is a deep learning algorithm that includes convolutional layers and has shown significant advantages in processing two-dimensional images (Deng, Ni, Bai, Jiang, & Xu, 2023; Ng et al., 2019). It is one of the representative algorithms of deep learning. As a data-driven modeling approach, CNN can extract useful information from high-dimensional raw spectra without the need for spectral preprocessing and feature extraction. CNN model can transform spectral data into abstract features through multiple layers of non-linear modules. Through layered feature extraction, the model can ultimately learn complex feature representations. In fact, CNN has been quite mature in the application of one-dimensional spectral analysis (Xue, Zhu, & Jiang, 2023), but its potential for two-dimensional spectral analysis has not been fully explored.

Upon careful consideration, the primary tasks of this research are outlined as follows: (1) Preparation of the colorimetric sensor array to obtain wheat with different levels of ZEN contamination; (2) Acquisition of near-infrared spectral data from the colorimetric sensor array after its reaction with wheat samples using a near-infrared spectrometer; (3) Application of the CNN for training and establishing a regression model on the two-dimensional data converted from near-infrared spectra; (4) Comparative analysis of the robustness and generalization performance of the constructed model with that of the partial least squares regression and support vector regression models.

2. Materials and methods

2.1. Collection and preparation of samples

For the investigation of ZEN content, a total of 5 kg naturally grown wheat grains acquired online shopping. They were placed in an incubator where the optimal conditions for ZEN toxin production are within a temperature range of 26 to 30 °C and a humidity range of 75 to 85 %. Random samples of 200 g were taken daily, and a grinder (BJ-150, Baijie Electrical Appliances Co., Ltd., Deqing, China) was employed to grind the wheat into powder to obtain a uniform sample. An electronic balance was used to divide the wheat powder into 12 portions, each weighing 10 g. Additionally, the equipment was thoroughly cleaned during daily sample collection to prevent contamination between samples. Following this procedure, sampling was conducted for eleven days, resulting in a total of 132 representative samples.

2.2. Detection of ZEN

In this study, the quantitative detection of ZEN toxin in wheat was conducted using a ZEN quantitative detection card. The principle of this detection card is based on competitive colloidal gold technology. Prior to toxin detection, stabilize all reagents and samples at room temperature. Subsequently, 2 g wheat samples were taken in test tubes, to which 8 ml of extraction reagent (70 % CH_3OH) was added. The test tubes were then placed in an oscillator and shaken for 3 min. Next, 1.5 ml of liquid was taken from the test tube into the eppendorf tube, which was centrifuged at 10,000 rpm for 1 min. Subsequently, 100 μL centrifugal supernatant was mixed with 900 μL diluent. After that, 100 μL of the mixture drops were rapidly pipetted into the sample well of the detection card, and the timing started. After 6 min, the results were read.

2.3. Preparation of colorimetric sensor array

The substrate material for the colorimetric sensor should possess good hydrophobicity and stability. Therefore, C2 reverse phase silica gel plate was selected as the substrate material. Based on the research team's prior investigations into the volatile gases from moldy wheat, porphyrin materials were initially chosen as color sensitive material of

sensing unit. Following preliminary experiments to observe the staining effect of porphyrin materials on silica gel plate, six porphyrin materials shown in Table 1 were ultimately selected to prepare the colorimetric sensor array.

The six types of porphyrin materials were separately dissolved in dichloromethane to prepare solutions with a concentration of 2 mg/mL, and sealed in brown bottles. The prepared six solutions were placed in an ultrasonic cleaner and oscillated for 15 min to ensure complete dissolution of the porphyrin materials. After preparation, the six solutions were stored at low temperature and shielded from light for later use. During the sensor preparation, approximately 1 μL of each solution was extracted using a capillary tube (0.3 × 100 mm), and sequentially spotted onto a 3 cm × 3 cm silica gel plate to create a 2 rows by 3 columns array of colorimetric spots for each solution. The prepared arrays were sealed in bags and stored for later use.

2.4. Acquisition of near-infrared data

The wheat samples, weighing 10 g, were placed into 60 mm diameter petri dishes, and the wheat flour was spread and compacted. Simultaneously, the base of the sensor array was fixed on a plastic film, which was used to seal the petri dishes, ensuring that the sensor array was positioned directly facing the wheat samples for a full reaction with the wheat volatiles for 20 min. Upon completion of the reaction, the spectral data for each colorimetric spot was immediately collected using a near-infrared spectroscopy acquisition system. The experiment utilized an integrating sphere to gather the reflectance of each colorimetric spot, with the spectrometer's integration time set at 100 ms, 3 scan averages, and a 5-point moving average width. Each acquired spectrum consisted of 128 data points. Fig. 1 displays the collected raw spectra.

The experiment collected a total of 132 samples, each yielding 128 spectra from six different colorimetric spots. In this study, the spectra corresponding to each sample were transformed into a two-dimensional format of 6 × 128.

2.5. Spectral data preprocessing

Preprocessing of spectral data is an important step in spectral analysis and interpretation. Savitzky-Golay (SG) is a linear smoothing technique widely used in the preprocessing of spectral data. It can be used to remove noise, smooth baseline, and reduce random fluctuations in the data, thus enhancing the accuracy of subsequent spectral analysis and interpretation. The advantage of SG is its ability to reduce noise while preserving spectral features. Additionally, it can control the degree of smoothing by adjusting the window size and polynomial order. In this study, the parameters for the window size and polynomial order of SG were set to 41 and 5, respectively.

2.6. Convolutional neural network

The more layers there are in a CNN model, the more complex features it can extract (Wang, Tian, Yang, Zhu, Jiang, & Cai, 2020). However, excessive depth increases model complexity, making training more difficult and increasing the risk of overfitting. Similarly, different convolutional kernels can extract various types of features. While a larger number of kernels can extract more features, an excessive number leads to model redundancy and increased computational load. Therefore, in the model design process, structural selection should be comprehensively considered based on the input dataset. Because of the limited data volume and the relatively low number of wavelengths in the input spectral data, the basic structure of the designed CNN model included 2 convolutional layers, 2 pooling layers, and 3 fully connected layers. The size of the kernels in the two convolutional layers was set to 3 × 3, with a quantity of 64. The neuron node numbers for the first and second fully connected layers were set at 64, using max-pooling for the pooling method. Since the model was for quantitative analysis, the number of output neuron nodes was set to 1. To prevent model overfitting and save training time, Gaussian noise was added before the input layer. Additionally, dropout layers were included between one pooling layer and the second convolutional layer, and between the two fully connected layers. Dropout layers temporarily ignored some neuron nodes at a certain probability during training, weakening the joint adaptability among neurons and preventing model overfitting. Fig. 2 illustrates the final CNN constructed for two-dimensional input in this study.

Table 1
Color sensitive materials in colorimetric sensor array.

Number	Name
1	5,10,15,20-Tetraphenyl-21H,23H-porphine
2	5,10,15,20-Tetraphenyl-21H,23H-porphine copper (II)
3	5,10,15,20-Tetrakis(4-methoxyhenyl)-21H,23H-porphine cobalt(II)
4	5,10,15,20-Tetraphenyl-21H,23H-porphine zinc
5	5,10,15,20-Tetraphenyl-21H,23H-porphine vanadium(IV) oxide
6	2,3,7,8,12,13,17,18-Octaethyl-21H,23H-porphine ruthenium(II) carbonyl

2.7. Partial least squares regression

The partial least squares regression (PLSR) method selects a linear combination of independent variables that are strongly correlated with the dependent variable and are computationally convenient (Leng, Li, Chen, Tang, Xie, & Yu, 2021). This approach effectively extracts comprehensive information that best explains the system, achieving dimensional reduction of high-dimensional data spaces. It can better overcome multicollinearity among variables, is more stable, and provides stronger interpretability. However, it cannot control overfitting during the learning process and lacks variable selection features. PLSR is a prevalent linear spectral analysis technique utilized to establish a linear relationship between spectral variables and the variables under consideration. PLSR effectively addresses the challenge of multicollinearity among independent variables. However, it is not suitable for cases where the spectral and measured variables exhibit complex nonlinear relationships due to the characteristics of spectral overlap and variation. In this study, a five-fold cross-validation was conducted to select the number of PLSR latent variables, ranging from 1 to 20.

2.8. Support vector machine regression

The support vector machine regression (SVR) model, derived from the support vector machine model, aims to identify relationships between independent and dependent variables in nonlinear regression problems (Z. Liu et al., 2022). By introducing a non-linear mapping function, datasets with non-linear regression relationships in low-dimensional space are mapped to high-dimensional space, followed by a transformation into a linear regression relationship. SVR exhibits strong generalization and wide adaptability. It is a powerful nonlinear model that can effectively capture the intricate relationships between the spectral variables and the target variables, resulting in accurate regression predictions. In this study, the radial basis function was employed as the kernel function, parameter 'c' balanced the model's complexity and fitting error, and parameter 'g' specified the influence of each sample on the model fitting. During SVR model training, grid search was utilized to select optimal values for 'c' and 'g', within a range from 2^{-10} to 2^{10}.

2.9. Software

The algorithms performed in this study were run on MATLAB R2021a and Jupyter Notebook with Python libraries installed.

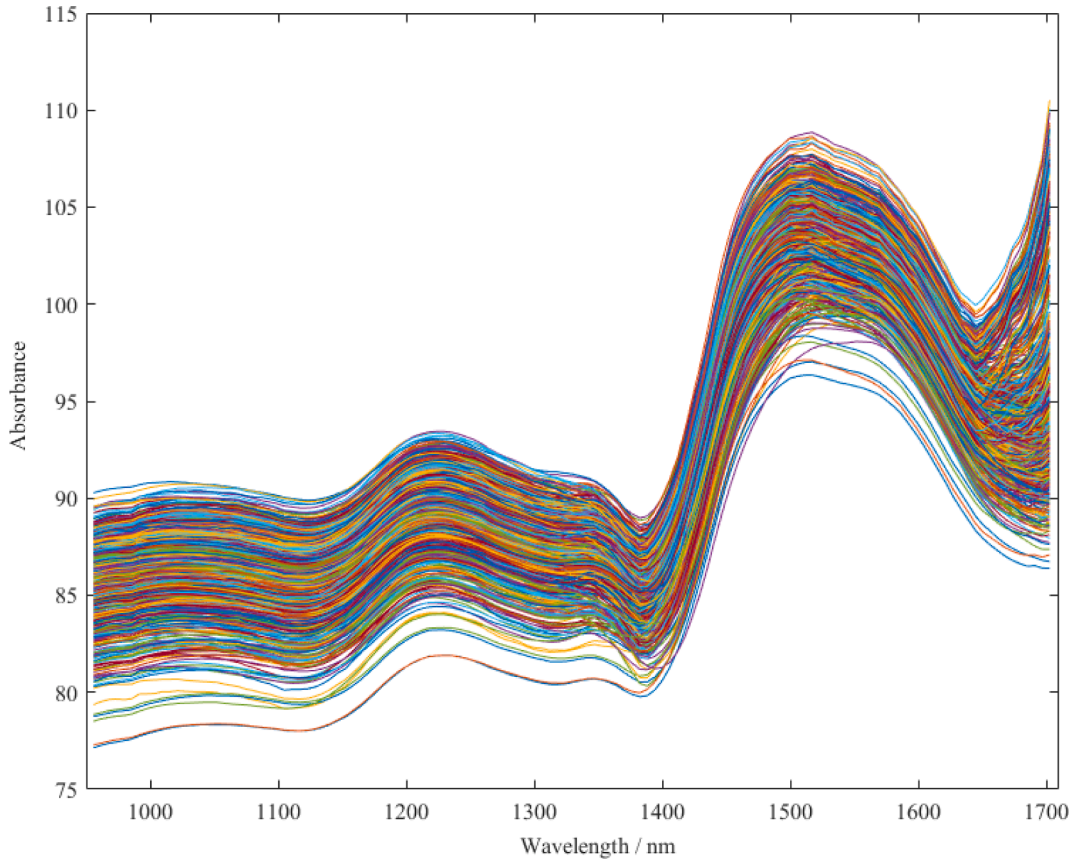

Fig. 1. Near-infrared spectra of colorimetric spots.

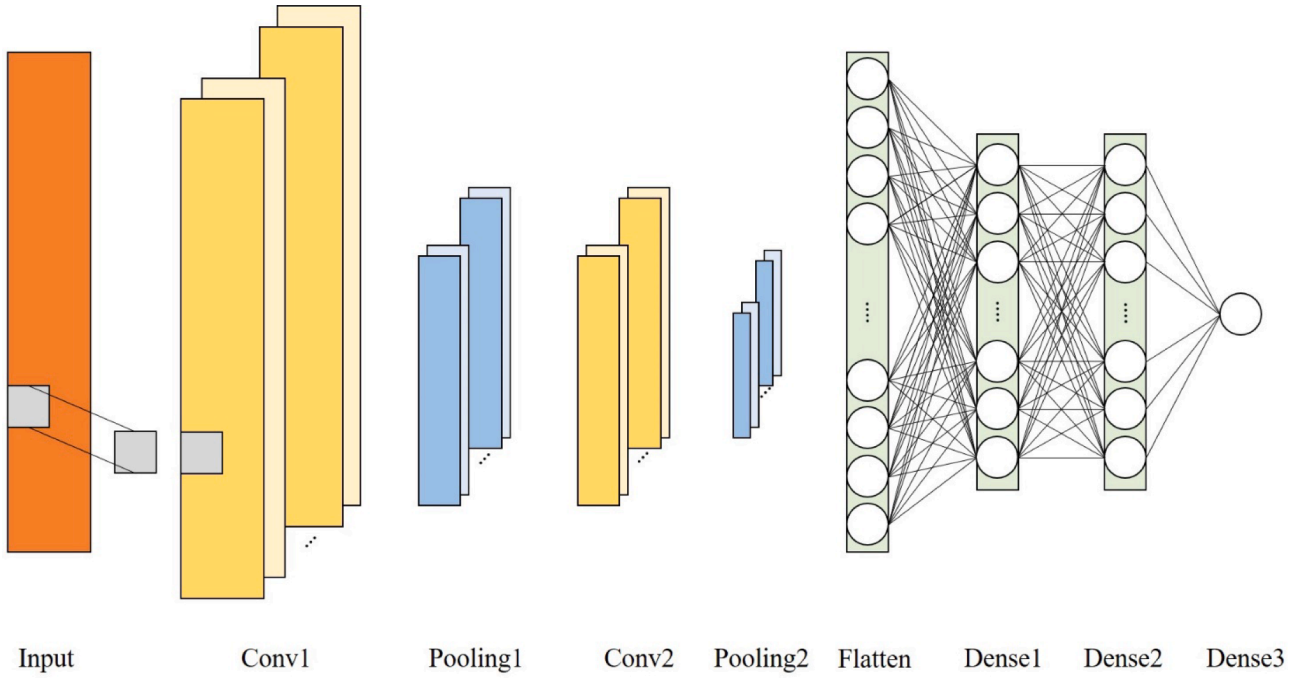

Fig. 2. Structure diagram of CNN model.

3. Results and discussion

3.1. Division of dataset

In this study, the dataset was initially randomly divided into a calibration set and a prediction set in approximately a 4:1 ratio, comprising 105 samples in the calibration set and 27 samples in the prediction set. The PLSR and SVR models were trained using the calibration set data. For CNN, the calibration set data was further randomly divided into a new training set and a validation set in a 4:1 ratio. The new training set contained 84 samples, and the new validation set contained 21 samples. The model weights were trained on the new training set, and the best hyperparameters were selected based on the model's performance on the validation set to determine the properly trained model. Subsequently, the predictive performance of the three models was tested on the prediction set after training. Table 2 presents the statistical results of the ZEN content of wheat samples in the calibration and validation sets.

3.2. The results of nonlinear detection

In this study, it was uncertain whether there is a nonlinear relationship between the spectral signal and the concentration of ZEN in wheat. Before the model was built, the runs test was used to check the serial correlation of the residuals (Centner, De Noord, & Massart, 1998). Table 3 shows the results of the nonlinear detection. The spectral signal of the colorimetric sensor array was not linear with the ZEN level in wheat. Therefore, SVR and CNN were used to establish the model in this study.

3.3. The results of CNN

In this study, the spectral data and ZEN reference values were initially globally scaled (GS) to enable the CNN model to capture features of different scales, thereby enhancing model performance. Both the spectral data and ZEN reference values have been scaled to a range with a mean of 0 and a standard deviation of 2. Subsequently, the two-dimensional 6 × 128 data was fed into the CNN for model training. Additionally, a Gaussian Noise of 0.01 was introduced into the CNN to improve its robustness and generalization capability. The loss function, which evaluates the error between the model's predicted values and actual values, plays a crucial role in model training. For the spectral analysis in this study, the mean squared error (MSE) was used as the loss function for quantitative analysis models. The training utilized an initial learning rate of 0.0005 with the Adam optimizer as the optimization algorithm. Furthermore, the batch_size for training was set to 30, and the training epochs were set to 500. During the training of the CNN model, all random seeds were fixed, and no repeated experiments were conducted. Fig. 3 illustrates the training process of the CNN constructed in this study. It is evident from the graph that with increasing training iterations, both the training and validation set's loss functions continuously decreased, indicating that the CNN was actively learning spectral data features during training. Further analysis revealed a significant decrease in the loss function curve within the first 200 epochs, followed by a more gradual and convergent trend beyond the 200th epoch. The marginal difference between the two curves indicates that the model did not overfit, signifying the success of the CNN training overall.

Table 3
The results of nonlinear detection.

n_+	n_-	u	μ	σ	$\|z\|$	Conclusion
386855.43	1323.41	1	585.63	258.02	36.37	Nonlinearity

3.4. Compare and discuss the results of different models

In this study, the spectral curves of the six colorimetric spots were sequentially connected to form a continuous spectral curve, which was then subjected to SG preprocessing. The preprocessed spectral data were used to establish PLSR and SVR models. Specifically, for the PLSR model, the optimal number of latent variables was determined through five-fold cross-validation using the calibration set data. As for the SVR model, a grid search algorithm was employed as the method for optimizing the SVM model parameters. Table 4 presents the results of different models, among them, the coefficient of determination on the prediction (R_p^2) of the CNN model was 0.91, the R_p^2 of the PLSR model was 0.77 and the R_p^2 of the SVR model was 0.68. The root mean square error of prediction (RMSEP) of the CNN model was 40.92μ g • kg^{-1},the RMSEP of PLSR model was 64.44μ g • kg^{-1} and the RMSEP of SVR model was 75.17μ g • kg^{-1}. It is evident that RMSEP of the CNN model was lower than that of the SVR and PLSR models, while its the R_p^2 was higher than both models.

The results indicated that the PLSR model performs poorly in both the calibration and prediction sets but did not exhibit clear signs of overfitting. This suggested that the PLSR model's ability to extract common features from the spectra was limited in datasets with higher sample diversity, resulting in poor performance in both the calibration and prediction sets. Moreover, the SVR model's coefficient of determination for the prediction set was only 0.68, indicating overfitting during the analysis process, leading to poor predictive results. In the CNN, the local perception ability of convolutional layers is advantageous for extracting peak and valley features in spectra. The shared convolutional kernel parameters reduce the quantity of parameters, accelerate learning rate, and prevent overfitting. The pooling layer continuously reduces the spatial size of the data in spectral processing, compressing the input feature maps and simplifying network computational complexity. Furthermore, pooling aids in feature compression, enabling extraction of the primary features in the spectra. Lastly, the deep structure of the CNN enhances the model's fitting and feature extraction capabilities, making it suitable for spectral analysis. The CNN model exhibited better predictive results compared to the SVR and PLS models, indicating its capability to capture underlying common features within the spectra of the six colorimetric spots, leading to improved accuracy. Overall, the CNN model demonstrated a clear advantage over traditional methods, indicating superior data fitting capabilities. This suggested that the CNN model's fitting performance excels particularly with more complex spectral sample datasets.

4. Conclusions

This study demonstrates that the combination of colorimetric sensor technology and near-infrared spectroscopy is an effective method for quantifying the ZEN content in wheat. Using six porphyrin materials, a simple structured colorimetric sensor array successfully captured the odor information of volatile compounds in wheat. Furthermore, this paper presented a two-dimensional CNN spectral quantification model that utilizes the original near-infrared spectral data from the six color-

Table 2
The results of the level of measured ZEN in wheat in CNN training.

Subsets	Number of samples	Units	Maximum	Minimum	Mean	Standard deviation
Calibration set	84	$\mu g.kg^{-1}$	483.96	22.96	100.19	129.17
Validation set	21	$\mu g.kg^{-1}$	401.44	20.24	67.62	94.71

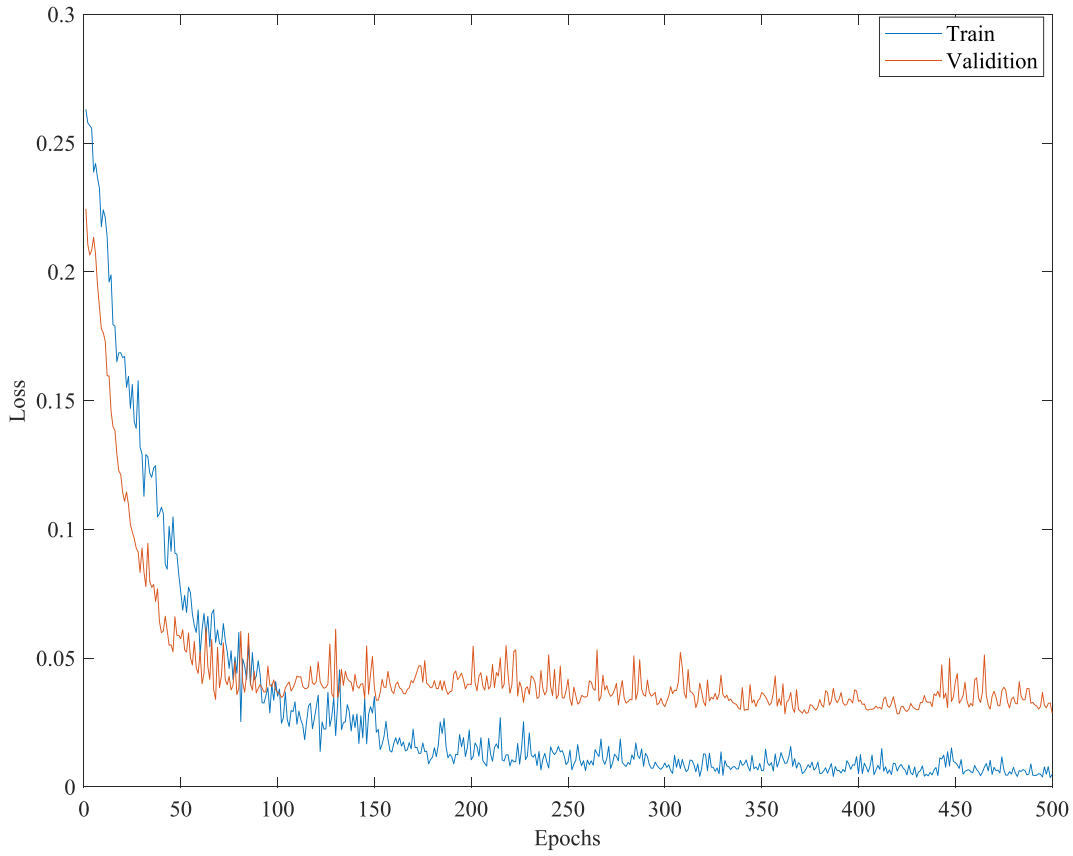

Fig. 3. The training results of the CNN.

Table 4
The results of different models.

Model	RMSEC/μ g • kg^{-1}	R_C^2	RMSEP/μ g • kg^{-1}	R_P^2
CNN	24.02	0.96	40.92	0.91
PLSR	57.22	0.78	64.44	0.77
SVR	35.91	0.91	75.17	0.68

imetric sensor points without preprocessing, leading to increased spectral analysis accuracy. A comparison of this model with the PLSR and SVR revealed that the CNN model achieved the lowest RMSEP of 40.92μ g • kg^{-1} and the best R_P^2 of 0.91. By integrating the spectral information of the colorimetric sensor points with the CNN for the prediction of wheat mycotoxins, this approach provided a new technological means for the rapid detection and safety monitoring of mycotoxins in wheat.

CRediT authorship contribution statement

Yongqin Zhao: Writing – original draft, Methodology. **Jihong Deng:** Writing – review & editing. **Quansheng Chen:** Methodology. **Hui Jiang:** Writing – review & editing, Project administration.

Declaration of competing interest

The authors declare that they have no known competing financial interests or personal relationships that could have appeared to influence the work reported in this paper.

Data availability

Data will be made available on request.

Acknowledgements

The authors gratefully acknowledge the financial support provided by the National Key Research and Development Program of China (Grant No. 2017YFC1600603), and the Postgraduate Research & Practice Innovation Program of Jiangsu Province (Grant No. KYCX22_3685).

References

Agriopoulou, S., Stamatelopoulou, E., & Varzakas, T. (2020). Advances in occurrence, importance, and mycotoxin control strategies: Prevention and detoxification in foods. *Foods, 9*(2), 137.
Arzani, A., & Ashraf, M. (2017). Cultivated ancient wheats (Triticum spp.): A potential source of health-beneficial food products. *Comprehensive Reviews in Food Science and Food Safety, 16*(3), 477–488.
Batrinou, A., Houhoula, D., & Papageorgiou, E. (2020). Rapid detection of mycotoxins on foods and beverages with enzyme-linked immunosorbent assay. *Quality Assurance and Safety of Crops & Foods, 12*(1), 40–49.
Bentley, A. R., Donovan, J., Sonder, K., Baudron, F., Lewis, J. M., Voss, R., & Saunders, D. G. (2022). Near-to long-term measures to stabilize global wheat supplies and food security. *Nature Food, 3*(7), 483–486.
Centner, V., De Noord, O., & Massart, D. (1998). Detection of nonlinearity in multivariate calibration. *Analytica Chimica Acta, 376*(2), 153–168.
Chen, X., Wu, H., Tang, X., Zhang, Z., & Li, P. (2023). Recent advances in electrochemical sensors for mycotoxin detection in food. *Electroanalysis, 35*(2), e202100223.
Deng, J., Ni, L., Bai, X., Jiang, H., & Xu, L. (2023). Simultaneous analysis of mildew degree and aflatoxin B1 of wheat by a multi-task deep learning strategy based on microwave detection technology. *Lwt, 184*, Article 115047.
Irakli, M. N., Skendi, A., & Papageorgiou, M. D. (2017). HPLC-DAD-FLD method for simultaneous determination of mycotoxins in wheat bran. *Journal of Chromatographic Science, 55*(7), 690–696.
Janik, E., Niemcewicz, M., Podogrocki, M., Ceremuga, M., Gorniak, L., Stela, M., & Bijak, M. (2021). The existing methods and novel approaches in mycotoxins' detection. *Molecules, 26*(13), 3981.
Jia, M., Pan, Y., Zhou, J., & Zhang, M. (2021). Identification of Chinese teas by a colorimetric sensor array based on tea polyphenol induced indicator displacement assay. *Food Chemistry, 335*, Article 127566.
Jiang, H., Deng, J., & Chen, Q. (2023). Olfactory sensor combined with chemometrics analysis to determine fatty acid in stored wheat. *Food Control*, Article 109942.

Leng, T., Li, F., Chen, Y., Tang, L., Xie, J., & Yu, Q. (2021). Fast quantification of total volatile basic nitrogen (TVB-N) content in beef and pork by near-infrared spectroscopy: Comparison of SVR and PLS model. *Meat Science, 180*, Article 108559.

Liu, T., Jiang, H., & Chen, Q. (2022). Input features and parameters optimization improved the prediction accuracy of support vector regression models based on colorimetric sensor data for detection of aflatoxin B1 in corn. *Microchemical Journal, 178*, Article 107407.

Liu, Z., Zhang, R., Yang, C., Hu, B., Luo, X., Li, Y., & Dong, C. (2022). Research on moisture content detection method during green tea processing based on machine vision and near-infrared spectroscopy technology. *Spectrochimica Acta Part A: Molecular and Biomolecular Spectroscopy, 271*, Article 120921.

Mishra, P., & Passos, D. (2021). A synergistic use of chemometrics and deep learning improved the predictive performance of near-infrared spectroscopy models for dry matter prediction in mango fruit. *Chemometrics and Intelligent Laboratory Systems, 212*, Article 104287.

Ng, W., Minasny, B., Montazerolghaem, M., Padarian, J., Ferguson, R., Bailey, S., & McBratney, A. B. (2019). Convolutional neural network for simultaneous prediction of several soil properties using visible/near-infrared, mid-infrared, and their combined spectra. *Geoderma, 352*, 251–267.

Pasquini, C. (2018). Near infrared spectroscopy: A mature analytical technique with new perspectives–A review. *Analytica Chimica Acta, 1026*, 8–36.

Ropejko, K., & Twarużek, M. (2021). Zearalenone and its metabolites—General overview, occurrence, and toxicity. *Toxins, 13*(1), 35.

Sadhasivam, S., Britzi, M., Zakin, V., Kostyukovsky, M., Trostanetsky, A., Quinn, E., & Sionov, E. (2017). Rapid detection and identification of mycotoxigenic fungi and mycotoxins in stored wheat grain. *Toxins, 9*(10), 302.

Sun, S., Qian, S., Zheng, J., Li, Z., & Lin, H. (2020). A colorimetric sensor array for the discrimination of Chinese liquors. *Analyst, 145*(21), 6968–6973.

Tahoun, I. F., Gab-Allah, M. A., Yamani, R. N., & Shehata, A. B. (2021). Development and validation of a reliable LC-MS/MS method for simultaneous determination of deoxynivalenol and T-2 toxin in maize and oats. *Microchemical Journal, 169*, Article 106599.

Varzakas, T. (2016). Quality and safety aspects of cereals (wheat) and their products. *Critical Reviews in Food Science and Nutrition, 56*(15), 2495–2510.

Wang, D., Tian, F., Yang, S. X., Zhu, Z., Jiang, D., & Cai, B. (2020). Improved deep CNN with parameter initialization for data analysis of near-infrared spectroscopy sensors. *Sensors, 20*(3), 874.

Xu, W., He, Y., Li, J., Deng, Y., Xu, E., Feng, J., & Wang, W. (2022). Non-destructive determination of beef freshness based on colorimetric sensor array and multivariate analysis. *Sensors and Actuators B: Chemical, 369*, Article 132282.

Xue, Y., Zhu, C., & Jiang, H. (2023). Comparison of the performance of different one-dimensional convolutional neural network models-based near-infrared spectra for determination of chlorpyrifos residues in corn oil. *Infrared Physics & Technology, 132*, Article 104734.

Zhao, M., Jiang, H., & Chen, Q. (2023). Identification of procymidone in rapeseed oils based on olfactory visualization technology. *Microchemical Journal, 193*, Article 109055.